Molecular Cell, Vol. 3, 629–638, May, 1999, Copyright ©1999 by Cell Press

Crystal Structures of c-Src Reveal Features of Its Autoinhibitory Mechanism

Wenqing Xu,*‡# Amish Doshi,§ Ming Lei,*‡ Michael J. Eck,‡§‖ and Stephen C. Harrison*†‡‖
*Laboratory of Molecular Medicine
Children's Hospital
†The Howard Hughes Medical Institute
300 Longwood Avenue
‡Department of Biological Chemistry and Molecular Pharmacology
Harvard Medical School
§Department of Cancer Biology
Dana-Farber Cancer Institute
44 Binney Street
Boston, Massachusetts 02115

Summary

Src family kinases are maintained in an assembled, inactive conformation by intramolecular interactions of their SH2 and SH3 domains. Full catalytic activity requires release of these restraints as well as phosphorylation of Tyr-416 in the activation loop. In previous structures of inactive Src kinases, Tyr-416 and flanking residues are disordered. We report here four additional c-Src structures in which this segment adopts an ordered but inhibitory conformation. The ordered activation loop forms an α helix that stabilizes the inactive conformation of the kinase domain, blocks the peptide substrate–binding site, and prevents Tyr-416 phosphorylation. Disassembly of the regulatory domains, induced by SH2 or SH3 ligands, or by dephosphorylation of Tyr-527, could lead to exposure and phosphorylation of Tyr-416.

Introduction

Protein kinases control so many aspects of cell growth, differentiation, and metabolism that their catalytic activities must be under tight control. Various modes of phosphorylation and inter- or intramolecular association regulate kinases in response to appropriate cellular stimuli. For example, cyclin-dependent kinases are controlled by their cyclins (De Bondt et al., 1993; Jeffrey et al., 1995; Morgan, 1995), Src family tyrosine kinases by their SH3 and SH2 domains (Superti-Furga and Courtneidge, 1995; Brown and Cooper, 1996; Sicheri et al., 1997; Xu et al., 1997; Williams et al., 1997), and cyclic-AMP-dependent kinase by interaction of cAMP with a regulatory subunit (Krebs, 1989; Taylor et al., 1990). Structural studies suggest that such diverse regulatory elements determine kinase activity by impinging upon just a few key components of the core kinase domain (Morgan and De Bondt, 1994; Johnson et al., 1996; Hubbard et al., 1998). These final common effectors are elements of the active site that contain catalytic or substrate-binding residues. They include the glycine-rich loop and helix C (termed the PSTAIRE helix in cyclin-dependent kinases) in the small lobe and the catalytic and activation loops in the large lobe. Modulation of the position and conformation of these elements by phosphorylation and by interaction with regulatory subunits can control catalytic activity. In addition, because active site residues are distributed between the N and C lobes of the kinase, changes in the relative orientation of the two lobes can turn the kinase on or off.

The activation loop, a segment of the large lobe of the kinase domain, has a particularly central role in catalytic regulation. Phosphorylation of this loop is required for full activity of many kinases. Crystal structures of active and inactive kinases show dramatic changes in the conformation of the activation loop upon phosphorylation (Russo et al., 1996; Yamaguchi and Hendrickson, 1996; Canagarajah et al., 1997; Hubbard, 1997). The unphosphorylated activation loops adopt divergent and often inhibitory conformations (Morgan and De Bondt, 1994; Johnson et al., 1996; Hubbard et al., 1998), and they autoinhibit the kinase either by disrupting the active site directly or by preventing substrate binding. For example, in the inactive insulin receptor tyrosine kinase, the activation loop threads through the active site, precluding binding of both ATP and protein substrates (Hubbard et al., 1994). In the FGF receptor kinase, the unphosphorylated loop blocks only the protein substrate–binding site (Mohammadi et al., 1996). In contrast, when phosphorylated, activation loops adopt similar conformations in all kinases studied to date. In this active conformation, the loop forms part of the recognition site for protein substrates (Johnson et al., 1996; Canagarajah et al., 1997; Hubbard et al., 1998).

Src family tyrosine kinases have multiple regulatory mechanisms, which converge on the common active site effectors. The domain structure of Src kinases includes a myristylated N-terminal "unique" domain, which differs among family members. This region is followed in the peptide chain by the SH3 domain, the SH2 domain, the tyrosine kinase domain, and a short C-terminal tail. Src activity is regulated by tyrosine phosphorylation at two sites with opposing effects. Phosphorylation of Tyr-416 in the activation loop of the kinase domain upregulates the enzyme; phosphorylation of Tyr-527 in the C-terminal tail renders the enzyme less active (Hunter, 1987; Superti-Furga and Courtneidge, 1995; Brown and Cooper, 1996). In vivo, the enzyme is phosphorylated at either Tyr-416 or Tyr-527, but not both.

Extensive biochemical and genetic characterizations have led to a model for Src regulation in which interaction of the phosphorylated C-terminal tail with the SH2 domain locks the molecule in an inhibited conformation (Matsuda et al., 1990). The SH3 domain has also been shown to be important for inactivation (Superti-Furga et al., 1993). Crystal structures of nearly full-length c-Src (Xu et al., 1997; Williams et al., 1997) and Hck (Sicheri

‖To whom correspondence should be addressed (e-mail: eck@red.dfci.harvard.edu [M. J. E.], schadmin@crystal.harvard.edu [S. C. H.]).
#Present address: Department of Biological Structure, Biomolecular Structure Center, University of Washington, Seattle, Washington 98195.

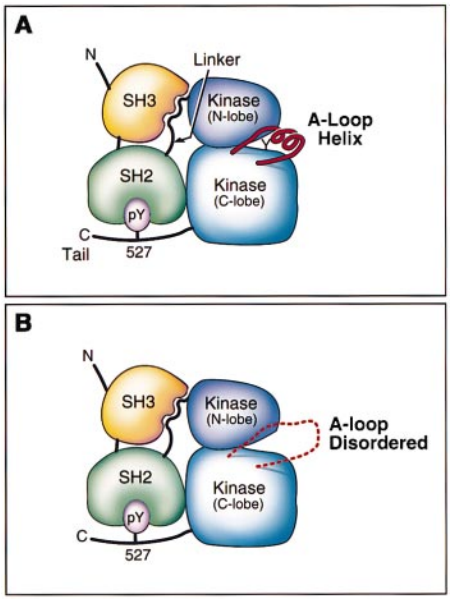

Figure 1. The Assembled Conformation of c-Src

Schematic illustrations of the human c-Src structures reported here and the previously determined human c-Src structure. In the Src-1 structure (b), the activation loop is disordered. In the structures of Src-2 to Src-5 (a), the activation loop forms an inhibitory helix. To accommodate this helix, the cleft between the two kinase lobes is about 5° more open than in the Src-1 structure.

et al., 1997) in the conformation stabilized by tail phosphorylation bear out many of the predictions of this model. The structures show that the phosphorylated tail binds intramolecularly with the SH2 domain, and that the SH3 domain interacts with the segment that links the SH2 domain and the N lobe of the kinase (Figure 1). The SH3 and SH2 domains pack against the N and C lobes, respectively, of the kinase domain, on the side opposite the catalytic cleft. Thus, inactivation of the enzyme does not involve covering of the catalytic site by the SH2 or the SH3 domain. Rather, assembly of the regulatory domains stabilizes a displacement of helix C, similar to the one observed for the PSTAIRE helix in cyclin-dependent kinases (De Bondt et al., 1993). This displacement removes a key residue (Glu-310 in Src) from the active site. Release of the SH3 and SH2 interactions and phosphorylation of Tyr-416 may all contribute to allowing helix C to adopt its catalytically competent position.

In the previously determined Src family structures, Tyr-416 and flanking residues near the center of the activation loop (defined as residues 404–432) are disordered (Sicheri et al., 1997; Xu et al., 1997; Williams et al., 1997; see Figure 1), and the ordered N- and C-terminal ends of the loop diverge from their conformations in the active forms of the insulin receptor (Hubbard, 1997) and Lck kinase domains (Yamaguchi and Hendrickson, 1996). We describe four additional structures of the inactive, tail-phosphorylated form of human c-Src, determined in the presence and absence of the ATP analog AMP–PNP and in two different crystal forms. In all these structures, the entire activation loop is ordered. It contains a helix (the "A loop helix") that packs between the upper and lower lobes of the catalytic domain, burying Tyr-416. The ordered conformation of the activation loop precludes binding of peptide substrates and protects Tyr-416 from phosphorylation. Our analysis of these structures and the buffer conditions in which they were determined leads us to conclude that the previously observed disorder in the activation loop was a result of stabilization of those crystals in high concentrations of glycerol, which slightly alters the relative orientation of the two lobes of the kinase domain. The structures described here suggest that sequestration of Tyr-416 may have an important function in maintaining the inactive state of the enzyme. We outline a model for activation of Src kinases, in which disassembly of the regulatory domains releases Tyr-416 and thereby promotes its phosphorylation.

Results and Discussion

Nomenclature

The structures of Src and Hck (Sicheri et al., 1997; Williams et al., 1997; Xu et al., 1997) illustrated in Figure 1 have "assembled regulatory domains" or an "assembled regulatory apparatus." We use these expressions here, rather than "closed state" or "closed, inactive conformation" (as introduced, for example, by Brown and Cooper [1996], and used in our earlier paper, Xu et al. [1997]) for the following reasons. First, we wish to avoid confusion with the use of "open" and "closed" to describe the catalytic cleft of the kinase. Second, because the Src and Hck structures show that the SH2–pTyr 527 interaction does not directly occlude the active site, but rather locks the regulatory domains in place on the side opposite the catalytic cleft, "restrained," rather than "closed" is probably a better description. Third, the lack of activity is due most directly to the position of helix C and the consequent absence of a properly configured catalytic site, and only indirectly to assembly of the regulatory domains. Indeed, the state of Src with assembled regulatory domains may not necessarily be inactive, provided that Tyr-416 is also phosphorylated (Boerner et al., 1996; Hardwick and Sefton, 1997).

Four New Crystal Forms of c-Src

We crystallized the inactive form of human c-Src (residues 83–533, phosphorylated on Tyr-527) bound with a nonhydrolyzable ATP analog, AMP–PNP. The structure, refined to an R factor of 22% using data to 1.8 Å resolution, reveals clear electron density for the AMP–PNP, as well as unexpected density corresponding to residues 413–418 in the c-Src activation loop (Figure 2). This portion of the activation loop forms an α helix, and the side chain of Tyr-416 extends from this helix toward the catalytic cleft. The corresponding segment was disordered in the previously described structures of Src family kinases with assembled regulatory domains. The structures reported here also have a slightly more open catalytic cleft than the earlier Src structures, due to a change in the relative orientation of the two lobes of the kinase domain.

The covalent structure of the protein in the present work, including its phosphorylation state, is the same as that used in the previous studies, but several crystallization and handling parameters varied. Our original c-Src crystal structure (which we will call "Src-1") was obtained in $\sim$1 M sodium tartrate with no ligand in the

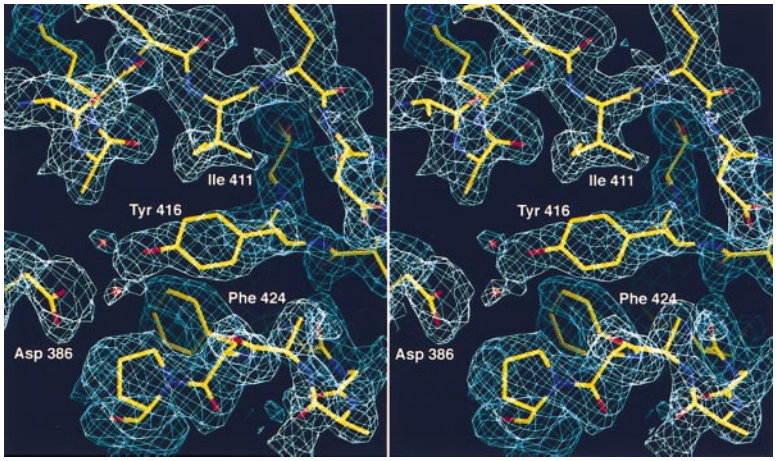

Figure 2. Stereo View of a Simulated Annealing Omit Map in the Region of the A Loop Helix, with the Refined Src-2 Atomic Model

Residues 411–423 were omitted. The map was calculated with coefficients $2F_o - F_c$ and contoured at 0.8 σ. The orientation is similar to that in Figure 3. Tyr-416 is buried, in part by hydrophobic interactions with Ile-411 and Phe-424. The hydroxyl group of Tyr-416 coordinates two water molecules (red spheres), which also hydrogen bond with buried polar groups on the catalytic loop.

nucleotide-binding pocket. These crystals were stabilized for 24 hr or more in 20% glycerol for data collection under low-temperature conditions. In contrast, the AMP–PNP complex described here crystallized in a different lattice with polyethylene glycol (PEG 4000) as a precipitant, and the crystals were exposed only briefly (less than 1 min) to glycerol prior to cryogenic data collection. In order to understand which of these variables affected the conformation of the activation loop, we determined three additional structures, in both high-salt (sodium tartrate) and low-salt (PEG 4000) conditions, and in both crystal lattices. A summary of the crystallization conditions and the structural analyses of Src-1, the AMP–PNP complex (Src-2), and the three additional forms (Src-3, -4, and -5) is presented in Table 1. In all four recently determined structures, residues 413–418 in the activation loop adopt the same helical conformation, and the relative orientations of the N- and C-terminal lobes of the tyrosine kinase domain are essentially the same. The ordered activation loop is present in both high- and low-salt conditions, with and without Mg-AMP-PNP, and in two different crystal lattices.

Comparison of Src-5 and Src-1 implicates glycerol soaking as a key variable. Src-5 crystals were grown in the same conditions as Src-1 but exposed to glycerol for less than 1 min as opposed to greater than 24 hr (Table 1). The helical conformation of residues 413–418 and the buried side chain of Tyr-416 are obvious in $2F_o - F_c$ electron density maps of Src-5 crystals calculated prior to inclusion of the activation loop in the model and also in "omit" maps. There is a reproducible lattice change in the tartrate crystal form during glycerol soaking (the "c" cell dimension decreases by $\sim$5 Å, and diffraction resolution improves from $\sim$3.0 Å to 1.5 Å). We conclude that stabilization of the crystals in glycerol pushes the two lobes of the kinase domain together and expels the activation loop. It is not clear whether glycerol has the same effect in solution; the changes in Src conformation may well be a consequence, rather than a cause, of the observed shrinkage in the crystal lattice. In any case, the crystal structures of Src-2, -3, -4, and -5 are likely to represent inactive c-Src in glycerol-free solution, since they come from two different crystal forms obtained with two very different precipitants. We refer to the conformation observed in the these structures as Src-2. Our description of the new conformation refers to the high-resolution AMP–PNP complex (Table 1, column 2), unless otherwise indicated.

Domain Orientations

The overall domain organization of all five c-Src crystal structures is basically the same (Figures 1 and 3), but the cleft between the two lobes of the kinase domain is about 5° more open in the four Src-2 Src structures than in Src-1. Comparison with other structures shows that

Table 1. Summary of Five c-Src Structures

	Crystal				
	Src-1	Src-2	Src-3	Src-4	Src-5
Ligands	None	AMP-PNP, (peptide)	None	None	None
Diffraction limits (Å)	1.5	1.8	2.5	2.8	3.25
Crystal packing type	I	II	II	I	I
Cell dimensions	a = 51.76 b = 87.38 c = 101.30	a = 50.59 b = 72.97 c = 172.69	a = 50.32 b = 72.75 c = 171.42	a = 51.14 b = 87.94 c = 106.09	a = 51.23 b = 86.66 c = 103.96
Crystallization Precipitant	Sodium tartrate	PEG 4000	PEG 4000	PEG 4000	Sodium tartrate
Crystal soaked for extended time in glycerol	Yes	No	No	No	No
Relative cleft opening[a]	−5.05°	0.33°	0.30°	−0.20°	−0.43°
Activation loop	Disordered	Helical	Helical	Helical	Helical

[a] Note: the average cleft opening of Src-2, -3, -4, and -5 was taken as zero; a minus sign indicates a more closed activation cleft.

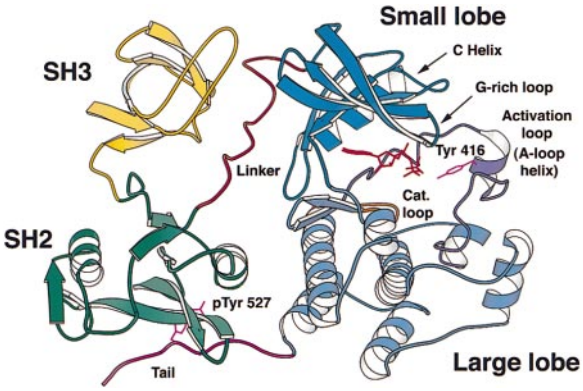

Figure 3. Ribbon Diagram Showing the Overall Organization of Src-2

The SH3 (yellow) and SH2 (green) domains coordinate the linker and phosphorylated tail segments, respectively. The tyrosine kinase domain is colored blue; AMP–PNP (red) is bound in the active site. The A loop helix packs between the N and C lobes of the kinase and sequesters Tyr-416.

the opening of this cleft can vary from kinase to kinase, even in what are believed to be corresponding states, probably because hinge motions can have somewhat different pivot points in each case and because crystal packing may affect observed lobe orientations. For example, the cleft opening in Src-2 is close to that found in the inactive form of cyclin-dependent kinase 2 (Cdk2) (De Bondt et al., 1993) and the active form of the cAMP-dependent protein kinase (Knighton et al., 1991; Zheng et al., 1993), and about 19° more closed than in the active Lck kinase domain (Yamaguchi and Hendrickson, 1996; see Figure 4b). Moreover, comparison of the ternary substrate complexes of the insulin receptor and cAMP-dependent kinases shows a signficant hinge–angle difference between the two molecules, both presumed to be in catalytically active conformations (Knighton et al., 1991; Hubbard, 1997). The conformation of the kinase domain in Src-2 is probably in part a consequence of its ordered activation loop, which may fix the relative orientation of the large and small lobes (Figure 4a). Indeed, the extraordinarily tight closure of the catalytic cleft in Src-1 is incompatible with the ordered activation loop seen in the new structures reported here. The distance between Cα atoms of Thr-301 and Thr-434, two residues roughly flanking either end of the activation loop helix, is 2.53 Å shorter in Src-1 than in Src-2.

The Activation Loop

The activation loop of c-Src includes residues 404–432. In the Src-1 structure, no electron density is observed for residues 410–423. In the Src-2 structures, the amino-terminal portion of the activation loop (residues 405–409) adopts a different conformation than the one seen in Src-1, and residues 413–418 in the previously disordered region form a short α helix (A loop helix), wedged between the two lobes of the catalytic domain. This conformation buries the side chain of Tyr-416, the positive regulatory site, between the lobes of the kinase domain. The average thermal parameter for residues

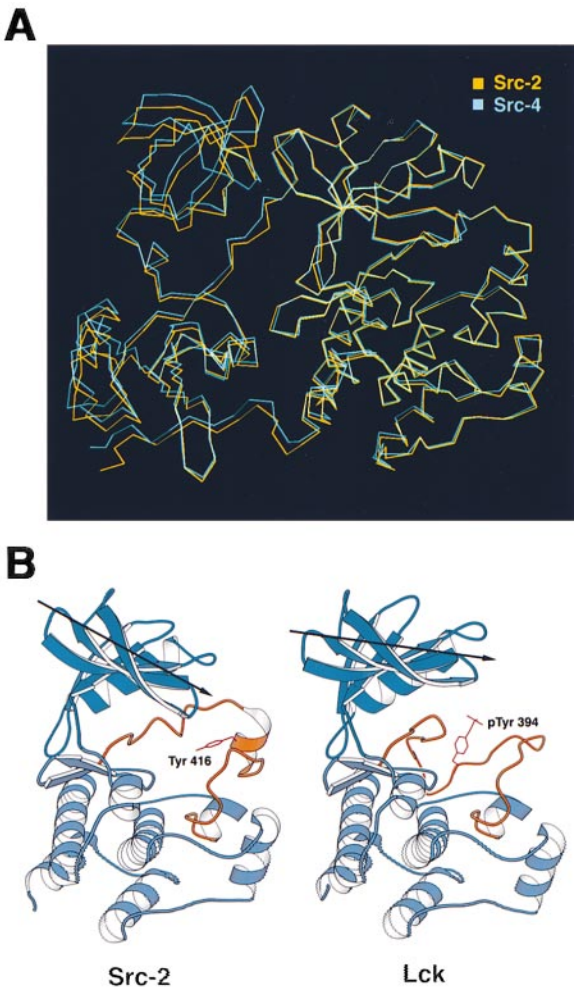

Figure 4. Domain Orientations in Src Family Kinases

(a) Comparison of two of the inactive structures reported here, viewed as in Figure 3. Src-2 (yellow) and Src-4 (cyan) have been superposed using the β strands in the small lobe of the kinase domain. The rest of the kinase, including the activation loop, also superposes well in this register; the regulatory domains shift slightly (probably due to crystal packing differences). The coordinate root-mean-square deviations (rmsd) of 261 kinase domain Cα atoms (residues 260–520) between Src-2 and Src-3, Src-4, and Src-5 are 0.32 Å, 0.50 Å, and 0.40 Å, respectively. The angle between the small and large lobes varies less than 0.8° among these four c-Src structures. The relative orientations of the SH3 domain and the small lobe, the SH2 domain and the large lobe, and SH3 and SH2 domains are slightly more variable. For example, between Src-2 and Src-4, the coordinate rmsd's for Cα atoms of the following domain–domain pairs are: the SH3 domain and the small lobe, 1.26 Å; the SH2 domain and the large lobe, 0.70 Å; and the SH3 and SH2 domains, 1.32 Å.

(b) Comparison of the inactive conformation of the Src-2 kinase domain and the active conformation of the Lck kinase domain (Yamaguchi and Hendrickson, 1996). The latter has a much more open catalytic cleft, as illustrated by the arrows across the small lobe. The direction of view is similar in both cases to Figure 3. Reorientation of helix C (at the rear of the small lobe) with respect to its β-strands is evident by noticing how the angle between its axis and the arrow changes. The inhibitory and active conformations of the activation loop (gold) are shown, with the side chain of Tyr-416 (and its counterpart, Tyr-394) in red.

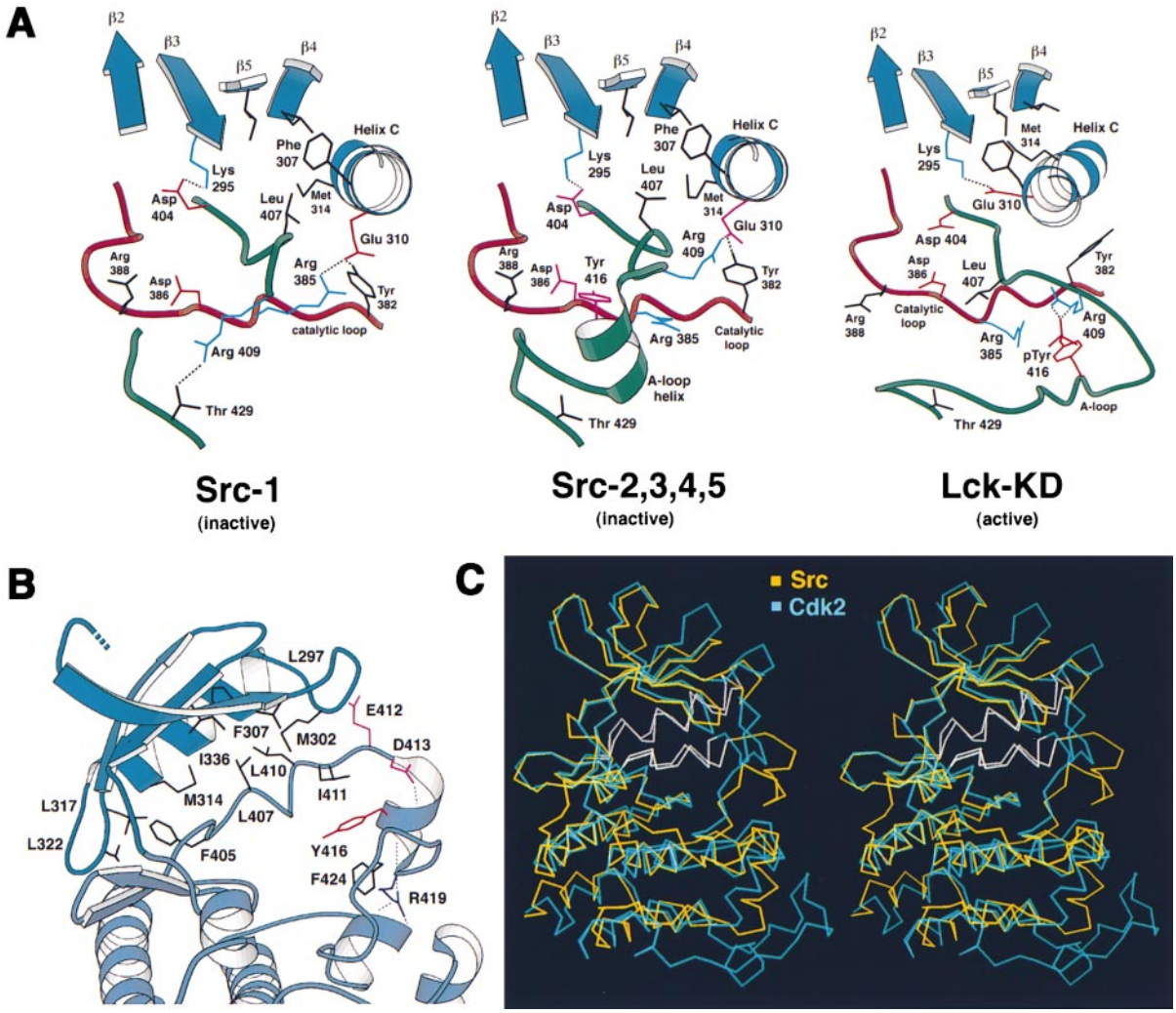

Figure 5. The Conformation of the Activation Loop of c-Src

(a) Three states of the active site, viewed into the cleft from the right of the molecule as oriented in Figures 1, 3, and 4. Portions of the small lobe are shown in blue; the catalytic loop is red; the activation loop is green. Src-1 and Src-2, -3, -4, and -5 are inactive. The Lck kinase domain is active (Yamaguchi and Hendrickson, 1996). Residues in the Lck structure have been renumbered to correspond to those in Src, in order to facilitate comparison. As in other active kinases, the conserved Glu-310 and Lys-295 in the Lck kinase domain form a critical salt bridge, positioning the Lys-295 side chain to coordinate the α- and β-phosphates of ATP. In the Src structures, this salt bridge is disrupted by displacement of the C helix, and access to the active site is also blocked by the N-terminal part of the activation loop (residues 404–410). The central part of the activation loop (residues 413–419) forms an inhibitory helix in Src-2,3,4 and -5, burying and protecting Tyr-416 and preventing formation of a substrate binding groove. In Src-1, residues 410–423 are disordered (break in the green tube). Note that the phosphate group on Tyr 416 (Src numbering) of the active Lck kinase domain forms salt bridges with Arg-385 and Arg-409, residues that interact with Glu-310 and stabilize the inactive orientation of the C helix in Src-1 and Src-2, respectively. Thus, phosphorylation of Tyr-416 appears to trigger an electrostatic switch, diverting Arg-385 and Arg-409 and promoting C helix reorientation.

(b) The hydrophobic interactions between the N-terminal part of the activation loop and the inward-facing surface of the C helix stabilize the inactive conformation. These hydrophobic interactions are supported by interactions between the A loop helix and each of the two kinase lobes and by hydrogen bonds between the Glu-312 side chain and the main chain of the loop between β3 and helix C. Mutation of two Pro residues in this loop renders Src completely deregulated by tail phosphorylation (Gonfloni et al., 1997). The C helix displacement is also stabilized by Trp-260 in the C-terminal end of the C helix (not shown here), as confirmed by mutagenesis studies (Gonfloni et al., 1997; LaFevre-Bernt et al., 1998). The orientation is the same as in Figures 3 and 4.

(c) Stereo view of a superposition of the inactive states of the Src and Cdk2 (De Bondt et al., 1993) kinase domains. The orientation is the same as in Figures 3 and 4. Src is in yellow; Cdk2 is in blue. The C helices and the N-terminal parts of the activation loops are in white. Note the similar positions and contacts of these two elements, despite the divergent conformations of the activation loops beyond the segment shown in white.

404–432 is 31 Å^2, essentially the same as for the overall structure (29 Å^2).

Residues 404–411 interact closely with the small lobe of the kinase domain (Figure 5b). This segment has a conformation very similar to the one adopted by the corresponding segment in the inactive form of human CDK2 (De Bondt et al., 1993; see Figure 5c). When the small lobes of Src and CDK2 are superposed, residues

404–411 of Src (DFGLARL) and residues 145–152 of CDK2 (DFGLARA) also coincide, with an rms Cα separation of 0.723 Å. The GLARA sequence in CDK2 is α-helical, and the corresponding sequence in Src has a 3_{10} helix conformation. In Src, Leu-407, Leu-410, and Ile-411 form a large hydrophobic interface with residues in the small lobe (Phe-278, Leu-297, Met-302, Phe-307, Met-314, and Ile-336; see Figure 5b); a similar hydrophobic contact is present in CDK2.

The conformation of residues 404–411 in Src-2 requires that helix C in the small lobe shift away from its position in an active kinase. As a result, Glu-310 in helix C of Src, a conserved residue that in active protein kinases forms a critical salt bridge with the catalytic lysine (Src residue 295), projects away from the catalytic site (Figures 5a and 6). The hydrophobic interactions just described, between the N-terminal part of the activation loop and the inward-facing surface of helix C, stabilize the inactive conformation. In addition, Arg-409 in the Src-2 structure forms a salt bridge with Glu-310. A precisely homologous interaction occurs in CDK2. Thus, in Src-2, the local interactions stabilizing the displacement of helix C are remarkably similar to those observed in CDK2. In Src-1, residues just beyond 409 are disordered, and Arg-409 extends into a pocket near Thr-429, rather than toward Glu-310. The partner of Glu-310 in Src-1 is Arg-385. The two conformations therefore have related but distinct mechanisms for excluding helix C and for stabilizing Glu-310 in its new position (Figure 5a).

The A loop helix forms a prominent bridge across the entrance to the catalytic cleft. The side chain of Asp-413 caps the N terminus of this helix, and the side chain of Arg-419 caps its C terminus. Arg-419 also caps the small helix, αEF, in the large lobe of catalytic domain, with hydrogen bonds to carbonyls 433–435. The side chain of Tyr-416 intercalates into a hydrophobic pocket formed by Phe-278 in the glycine-rich loop of the small lobe, Ile-411 in the first part of activation loop, and Phe-424 and Pro-425 in the large lobe (Figures 2 and 5b). The hydroxyl group of Tyr-416 coordinates two buried water molecules, which in turn also hydrogen bond with the catalytic loop. Thus, mutation of Tyr-416 to Phe could destabilize the A loop helix and partially activate the kinase (see also remarks on the differences between Phe-416 and unphosphorylated Tyr-416 in Brown and Cooper [1996]). The interactions around Tyr-416 probably stabilize a closed conformation of the kinase domain by helping to fix the relative orientation of its small and large lobes. Further, the presence of the A loop helix precludes protein substrate recognition in two respects. First, the helix physically occupies the space where peptide substrates should bind. Second, helix formation stabilizes the activation loop in a conformation in which the peptide recognition site is not fully formed. Thus, the A loop helix appears to be an important autoinhibitory element: it probably stabilizes the conformation of the kinase domain; it precludes peptide substrate recognition; and it sequesters Tyr-416, thereby preventing "inappropriate" activation by Tyr-416 phosphorylation. The helix is likely to be present in most inactive Src family kinases; the sequence of the activation loop and the residues that interact with it are conserved in known Src family members except Fgr. A corresponding feature has been seen in recent crystallographic studies of modified Hck (Schindler et al., 1999, this issue of *Molecular Cell*).

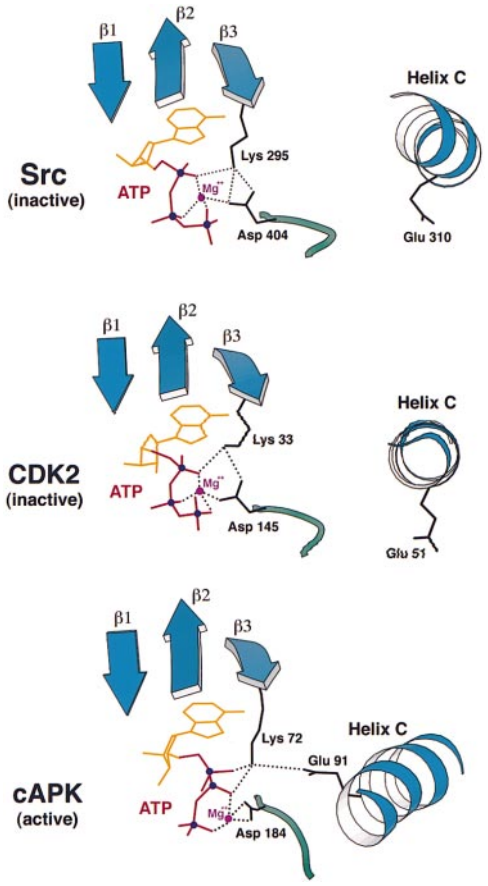

Figure 6. The Displacement of Helix C in Src Results in a Nonproductive Alignment of the ATP Phosphate Groups

This effect is also seen in Cdk2. Structures of Src-2, Cdk2 (De Bondt et al., 1993), and cAPK (cyclic-AMP-dependent kinase) (Knighton et al., 1991; Zheng et al., 1993) are shown in similar orientations (the same view as in Figure 5a), with the nucleoside colored orange and the phosphate groups and a critical magnesium ion colored red. In the active cAPK structure, the interaction between Glu-91 and Lys-72 allows the lysine side chain to interact with both the α- and β-phosphate groups, while the coordination between the conserved Asp-184 and a magnesium ion aligns the β- and γ-phosphate groups for nucleophilic attack. In both Src and Cdk2 structures, the displacement of helix C removes the critical glutamic acid residue, leaving the conserved lysine residue to interact with the α-phosphate only. The β-phosphate group is now far from its active position. The ATP conformation in the Src active site is modeled using that of AMP–PNP in the Src-2 structure.

The ATP-Binding Site

Except for the γ-phosphate group, the conformation of the bound AMP–PNP is well defined in Src-2. Although the γ-phosphate is poorly ordered, it is clear from the position of the β-phosphate group that the orientation of the scissile bond in Src-2 differs from that observed in structures of active protein kinases, including IRTK and the CDK2–cyclin complex (Figure 6). A single Mg^{2+} ion is octahedrally coordinated by all three phosphate groups of AMP–PNP, by Asn-391 and Asp-404, and by a water molecule. Lys-295 interacts with the α-phosphate

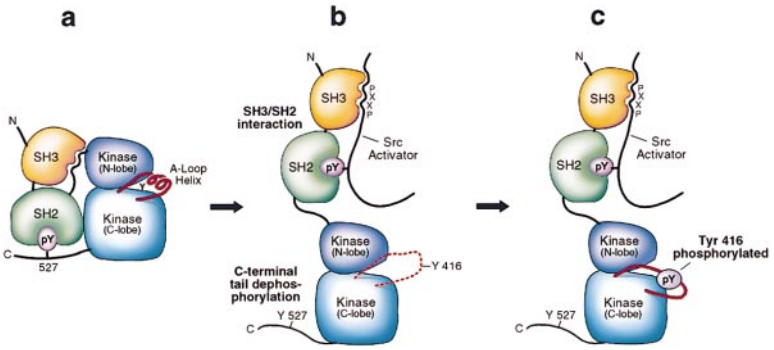

Figure 7. A Model for Src Activation

(a) The restrained conformation of c-Src is stabilized by intramolecular interactions among the kinase domain, the SH2/SH3 domains, and the phosphorylated C-terminal tail. In this state, an inhibitory conformation of the activation loop helps disrupt the kinase active site by stabilizing a displacement of the C helix. The formation of the A loop helix, which interferes with substrate binding and protects Tyr-416 from phosphorylation, relies on a particular register of the two kinase lobes.

(b) Displacement of SH2 and/or SH3 domains, either by C-terminal tail dephosphorylation or by competitive binding of optimal SH2/SH3 domain ligands, allows the kinase domain to open, disrupting the A loop helix and exposing Tyr-416 to phosphorylation.

(c) Phosphorylation of Tyr-416 initiates a conformational reorganization of the whole activation loop, relieving the steric barrier for substrate binding, allowing the C-terminal helix to move back into the active site, and reconstituting a fully active tyrosine kinase.

group rather than the α- and β-phosphate groups (its partners in active kinase structures). As in Src-1, the conformation of Lys-295 appears to be stabilized by its interaction with Asp-404. This salt bridge effectively "replaces" the Lys-295-Glu-310 interaction. The conformation of AMP–PNP, the coordination of the Mg^{2+} ion, and the interaction of Lys-295 are all extremely similar to homologous features in the inactive CDK2/ATP complex (Figure 6).

Implications for Src Activation

Src-2 shows a thoroughly inhibited molecule, in which self-consistent, intramolecular interactions cooperatively promote a conformationally restrained state. The SH3 and SH2 domains are turned inward; their targeting/recognition surfaces are occupied by intramolecular interactions with the linker and tail, respectively. They stabilize the two lobes of the kinase domain in a relative orientation that promotes the inhibitory conformation of the activation loop and that displaces helix C with a consequent disruption of the active site. In this state, Tyr-416 is unavailable for phosphorylation, and the substrate-binding site is not formed (Figure 7).

The mechanism by which the regulatory domains stabilize the observed conformation of the kinase is likely to involve a large number of contributing interactions. One specific suggestion has pointed to the position of Trp-260, at the junction between linker and kinase (Sicheri et al., 1997). Its side chain rests against helix C in its inactive position in Hck and Src and shifts away in the active conformation of Lck (Yamaguchi and Hendrickson, 1996). We believe that the structure described here is more consistent with a primary role for the N-terminal segment of the activation loop (residues 405–409) in expelling helix C. We suggest that the Trp-260 contact is one of several that link assembly of the regulatory apparatus with stability of a particular kinase conformation. We note, moreover, that assembly of the regulatory domains may be compatible with some catalytic turnover. Doubly phosphorylated c-Src, with phosphotyrosines at both 416 and 527, has significant activity (Boerner et al., 1996; Hardwick and Sefton, 1997). One plausible structural picture is that the activation loop rearranges in response to phosphorylation of 416 and that opening of the catalytic cleft and rotation of helix C can both occur without completely releasing the SH2 domain from the tail and the SH3 domain from the linker. In other words, the structures show that the assembled regulatory apparatus restrains the kinase domain, thereby contributing to sequestration of Tyr-416, but the assembled state may also be consistent with an active conformation at the catalytic site (provided that phosphorylation of Tyr-416 enforces the rearrangement). It is, however, possible that the catalytic activity present in the doubly phosphorylated kinase is due, at least in part, to a shift in the equilibrium between the assembled and disassembled conformations of the molecule. That is, the "local" rearrangements induced by phosphorylation of Tyr-416 may destabilize the restrained structure sufficiently to induce release of the regulatory domains. Efforts to crystallize the doubly phosphorylated form are continuing in our laboratory.

How are Src kinases activated? Interaction of the SH3 and SH2 domains with binding partners effectively "unbridles" the kinase domain (Figure 7). Src is known to be activated by SH2-mediated interaction with the autophosphorylated PDGF receptor (Erpel and Courtneidge, 1995), and by dual SH3/SH2 interactions with sequences in the focal adhesion kinase FAK (Thomas et al., 1998) and Sin (Alexandropoulos and Baltimore, 1996). These high-affinity binding partners outcompete the low-affinity intramolecular interactions, thereby disrupting the assembled quaternary structure. Because Tyr-416 and the A loop helix are packed between the two lobes of the kinase and are stabilized by interactions with both, we expect that release of the SH3 and SH2 interactions with the kinase domain will disorder the helix and effectively "present" Tyr-416 for phosphorylation. No direct structural data are available for this intermediate conformation, but it is likely to have a flexible and exposed activation loop (residues 410–423). The conformation of the N-terminal segment of the activation loop (residues 404–410) and the nonproductive orientation of helix C seen in Src-1 might also apply to this intermediate state. An alternative model is that disruption of the assembly of regulatory domains will allow helix C to rotate inward, reconstituting the kinase active site. In our view, this model is less satisfactory. The electrostatic switch described in the next paragraph suggests that Tyr-416 phosphorylation is likely to be a major factor in shifting

Table 2. Data Collection and Refinement

	Crystal			
	Src-2	Src-3	Src-4	Src-5
Data Collection				
Resolution	20.0–1.8	20.0–2.45	25.0–2.8	25.0–3.25
R_{sym}	5.1	5.5	6.1	8.2
Total observations	296913	51908	53552	25412
Unique reflections	55186	22372	11864	7639
Coverage	93.2	93.8	95.3	99.4
Refinement				
Resolution	20.0–1.8	20.0–2.5	20.0–2.8	20.0–3.25
R_{free}	28.1	30.8	31.0	32.1
R_{cryst}	22.6	21.8	26.8	27.1
Number of residues/<B>	450/29.28	452/19.90	450/28.71	452/69.31
Number of waters/<B>	299/39.77	236/21.46	23/35.22	0
rmsd bonds	0.007 Å	0.013 Å	0.005 Å	0.019 Å
rmsd angles	1.27°	1.56°	1.11°	1.99°
rmsd B values	2.83	1.14	2.82	2.69

$R_{sym} = \Sigma|I - <I>|/\Sigma I$, where I is the observed intensity and <I> is the average intensity of multiple observations of symmetry-related reflections.
$R = \Sigma||F_o| - |F_c||/\Sigma|F_o|$, where R_{free} is calculated for a randomly chosen 5% of reflections and R_{cryst} is calculated for the remaining 95% of reflections used for structure refinement.

the equilibrium to the active state. Direct structural analysis of Src unphosphorylated at Tyr-527 might provide a more definitive answer.

Upon phosphorylation of Tyr-416, the exposed, flexible activation sequence will probably adopt a new and well-defined conformation very similar to the one observed in the active forms of Lck and IRTK kinases. In active IRTK (Hubbard, 1997), the reordered activation loop forms two strands, one of which makes β sheet interactions with the bound substrate peptide. The phosphorylated activation loop of Lck (Yamaguchi and Hendrickson, 1996) also forms two short strands that pack against the large lobe of the kinase, pinned in place by coordination of the phosphorylated Tyr-416 with two arginine residues, Arg-385 and Arg-409 (we use Src residue numbers for simplicity; see Figure 5a). These are precisely the arginines that salt-bridge with Glu-310 in the Src-1 and Src-2 structures, respectively, to stabilize the inactive position of helix C. Thus, phosphorylation of Tyr-416 triggers an electrostatic switch, diverting arginines 385 and 409 and promoting reorientation of helix C. Additionally, in order for helix C to rotate inward, the N-terminal portion of the activation loop must reorient to relieve the steric hindrance. The corresponding portions of this loop in the active Lck and IRTK structures assume a conformation that does not block helix C, and residues 404–410 in active Src are likely to have a similar conformation. The net effect of these rearrangements is an active tyrosine kinase, competent to bind peptidic substrates and catalyze phosphotransfer.

In summary, we propose that the inhibitory conformation of the activation loop and its destabilization by phosphorylation of Tyr-416 link assembly and disassembly of the SH3-SH2 regulatory apparatus with events at the active site. The assembled regulatory domains, locked in place by insertion of Tyr-527 into the SH2 pocket, restrain the kinase domain and prevent a transient exposure of Tyr-416 that would favor its phosphorylation. The more prone the protein is to "breathe," the more likely it is to be activated.

Experimental Procedures

Crystallization and Data Collection

The human c-Src protein, homogeneously phosphorylated on Tyr-527, was produced using an insect cell expression system as previously described (Xu et al., 1997). The expressed fragment includes residues 86–536 of human Src (which corresponds to residues 83–533 of chicken Src). The purified protein was concentrated to 15 mg/ml in storage buffer (20 mM HEPES [pH 7.6], 0.1 M NaCl, and 5 mM DTT). Protein aliquots were frozen in liquid nitrogen and stored at −80°C. All crystals were obtained using the hanging drop method at room temperature. For Src-2 crystallization, 10 μl of thawed protein solution was combined with 1 μl of 0.1 M AMP–PNP and 2 μl of a potential substrate peptide (22 mM DEEIYGEFD peptide in 0.1 M Tris [pH 8.2] buffer). Src-2 crystals were grown in hanging drops by combining 1–2 μl above solution with 1 μl reservoir solution (50 mM MES [pH 6.5], 10 mM $MgCl_2$, 10 mM DTT, 8% PEG 4000). The peptide did not incorporate into the crystals. Both Src-3 and Src-4 crystals were obtained by combining 1–2 μl thawed c-Src protein solution with 1 μl reservoir solution containing 50 mM PIPES (pH 6.5), 10% PEG 4000, and 10 mM DTT. Src-5 crystals were grown with a reservoir solution containing 50 mM PIPES (pH 6.5), 0.8 M sodium tartrate, and 20 mM DTT. All Src crystals typically grew in ~2 days to a maximum size of $0.25 \times 0.25 \times 0.7$ mm^3. Crystals grown from PEG solution tend to form clusters, and microdissections were performed to isolate single crystals. For low-temperature data collection, all Src crystals were briefly "dunked" (less than 1 min) in a high glycerol solution, and then frozen immediately in a −160°C nitrogen gas stream. Src-2, -3, and -4 crystals were dunked in 25 mM PIPES or MES (pH 6.5), 20% PEG 4000, 22.5 % glycerol, 0.1 M NaCl, and 1 mM DTT. Src-5 crystals were dunked in 20 mM PIPES (pH 6.5), 1.15 M sodium tartrate, 20% glycerol, and 0.1 M NaCl. All Src crystals belong to space group $P2_12_12_1$, with one molecule in the asymmetric unit. Unit cell constants for each crystal form are shown in Table 1. Diffraction data from Src-3, Src-4, and Src-5 crystals were recorded with a Mar Research image plate scanner mounted on an Elliot GX-13 rotating anode source with mirror optics. The Src-2 data set was collected with a Fuji image plate system at the CHESS F-1 beamline (Cornell University). Diffraction data were integrated and scaled with the programs DENZO and SCALEPACK (Otwinowski, 1993) or MARXDS and MARSCALE (Kabsch, 1988).

Structure Determination and Refinement

The Src-2 and Src-3 structures were determined by molecular replacement with the program AmoRe (Navaza, 1992) using the Src-1 structure as a search model. Rotation and translation solutions calculated with the Src-3 data were unambiguous. The properly positioned model was subjected to overall and four-body rigid body

refinement (SH2/tail, SH3/linker, kinase N lobe, and kinase C lobe as rigid units) using XPLOR (Brünger, 1992). After a round of positional and B factor refinement, the Src-3 model was used as an initial model for Src-2. The Src-2 and c-Src-3 structures were then independently rebuilt and refined with reference to $2F_o - F_c$ and $F_o - F_c$ difference maps and simulated annealing omit maps. Electron density corresponding to the ordered activation loop was obvious in initial Src-2 maps, and the activation loop was built after a first cycle of model rebuilding with O (Jones et al., 1989) and crystallographic refinement with XPLOR. In the lower resolution Src-3 structure, the activation loop was constructed in the final stages of refinement. The models were further refined with simulated annealing and positional refinement, and manual rebuilding, with the programs XPLOR and O, respectively. Water molecules were added with the aid of the program ARP (Lamzin and Wilson, 1993).

The Src-4 and Src-5 structures were built by rigid body refinement of the Src-1 model, using XPLOR as outlined above. The Src-4 and Src-5 models were rebuilt and refined separately, with a combination of manually refitting with O and positional and restrained B factor refinement with XPLOR. Refinement statistics for all four structures are given in Table 2. There are no residues with disallowed main chain torsion angles. The main chain densities are well defined in all four structures, except for residues 521–525 and 530–533 in the C-terminal tail.

Illustration

The program O (Jones et al., 1989) was used to prepare Figures 2, 4a, and 5c; MOLSCRIPT (Kraulis, 1991) was used to create Figures 3, 5a, 5b, and 6.

Acknowledgments

We are especially grateful to Byron Ellis, Renee Boerner, Kevin Blackburn, W. Blaine Knight, and Michael Milburn of Glaxo-Wellcome for providing the c-Src(ΔN85) insect cell pellet used to prepare protein, for mass spectroscopic analysis, and for many helpful discussions. We thank K. Svenson for technical assistance, M. Lawrence and the staff at CHESS for help with synchrotron data collection, and B. Mayer for helpful discussions.

W. X. is a postdoctoral fellow supported by the Irvington Institute for Immunological Research. M. J. E. is the recipient of a Burroughs-Wellcome Fund Career award in the Biomedical Sciences. S. C. H. is an Investigator in the Howard Hughes Medical Institute. M. J. E. and S. C. H. are members of the Harvard-Armenise Center for Structural Biology at Harvard Medical School.

Received December 10, 1998; revised March 2, 1999.

References

Alexandropoulos, K., and Baltimore, D. (1996). Coordinate activation of c-Src by SH3- and SH2- binding sites on a novel p130CAS-related protein, Sin. Genes Dev. *10*, 1341–1355.

Boerner, R.J., Kassel, D.B., Barker, S.C., Ellis, B., DeLacy, P., and Knight, W.B. (1996). Correlation of the phosphorylation states of pp60 c-src with tyrosine kinase activity: the intramolecular pY530-SH2 complex retains significant activity if Y419 is phosphorylated. Biochemistry *35*, 9519–9525.

Brown, M.T., and Cooper, J.A. (1996). Regulation, substrates and functions of src. Biochim. Biophys. Acta *1287*, 121–149.

Brünger, A. (1992). X-PLOR Version 3.0: a System for Crystallography and NMR (New Haven, CT: Yale University Press).

Canagarajah, B.J., Khokhlatchev, A., Cobb, M.H., and Goldsmith, E.J. (1997). Activation mechanism of the MAP kinase ERK2 by dual phosphorylation. Cell *90*, 859–869.

De Bondt, H.L., Rosenblatt, J., Jancarik, J., Jones, H.D., Morgan, D.O., and Kim, S.H. (1993). Crystal structure of cyclin-dependent kinase 2. Nature *363*, 595–602.

Erpel, T., and Courtneidge, S.A. (1995). Src family protein tyrosine kinases and cellular signal transduction pathways. Curr. Opin. Cell Biol. *7*, 176–182.

Gonfloni, S., Williams, J.C., Hattula, K., Weijland, A., Wierenga, R.K., and Superti-Furga, G. (1997). The role of the linker between the SH2 domain and catalytic domain in the regulation and function of Src. EMBO J. *16*, 7261–7271.

Hardwick, J.S., and Sefton, B.M. (1997). The activated form of the Lck tyrosine protein kinase in cells exposed to hydrogen peroxide is phosphorylated at both Tyr-394 and Tyr-505. J. Biol. Chem. *272*, 25429–25432.

Hubbard, S.R. (1997). Crystal structure of the activated insulin receptor tyrosine kinase in complex with peptide substrate and ATP analog. EMBO J. *16*, 5572–5581.

Hubbard, S.R., Wei, L., Ellis, L., and Hendrickson, W.A. (1994). Crystal structure of the tyrosine kinase domain of the human insulin receptor. Nature *372*, 746–754.

Hubbard, S.R., Mohammadi, M., and Schlessinger, J. (1998). Autoregulatory mechanisms in protein-tyrosine kinases. J. Biol. Chem. *273*, 11987–11990.

Hunter, T. (1987). A tail of two src's: mutatis mutandis. Cell *49*, 1–4.

Jeffrey, P.D., Russo, A.A., Polyak, K., Gibbs, E., Hurwitz, J., Massague, J., and Pavletich, N.P. (1995). Mechanism of CDK activation revealed by the structure of a cyclinA-CDK2 complex. Nature *376*, 313–320.

Johnson, L.N., Noble, M.E., and Owen, D.J. (1996). Active and inactive protein kinases: structural basis for regulation. Cell *85*, 149–158.

Jones, T.A., Bergdoll, M., and Kjeldgaard, M. (1989). In Crystallographic Computing and Modeling Methods in Molecular Design, C. Bugg and S. Ealick, eds. (New York: Springer).

Kabsch, W. (1988). Evaluation of single crystal diffraction data from a position sensitive detector. J. Appl. Crystallogr. *21*, 916–924.

Knighton, D.R., Zheng, J.H., Ten, E.L., Ashford, V.A., Xuong, N.H., Taylor, S.S., and Sowadski, J.M. (1991). Crystal structure of the catalytic subunit of cyclic adenosine monophosphate-dependent protein kinase. Science *253*, 407–414.

Kraulis, P.J. (1991). MOLSCRIPT: a program to produce both detailed and schematic plots of protein structures. J. Appl. Crystallogr. *24*, 946–950.

Krebs, E.G. (1989). The Albert Lasker medical awards. Role of the cyclic AMP-dependent protein kinase in signal transduction. JAMA *262*, 1815–1818.

LaFevre-Bernt, M., Sicheri, F., Pico, A., Porter, M., Kuriyan, J., and Miller, W.T. (1998). Intramolecular regulatory interactions in the Src family kinase Hck probed by mutagenesis of a conserved tryptophan residue. J. Biol. Chem. *273*, 32129–32134.

Lamzin, V.S., and Wilson, K.S. (1993). Automated refinement of protein models. Acta Crystallogr. D *49*, 129–147.

Matsuda, M., Mayer, B.J., Fukui, Y., and Hanafusa, H. (1990). Binding of transforming protein, P47gag-crk, to a broad range of phosphotyrosine-containing proteins. Science *248*, 1537–1539.

Mohammadi, M., Schlessinger, J., and Hubbard, S.R. (1996). Structure of the FGF receptor tyrosine kinase domain reveals a novel autoinhibitory mechanism. Cell *86*, 577–587.

Morgan, D.O. (1995). Principles of CDK regulation. Nature *374*, 131–134.

Morgan, D.O., and De Bondt, H.L. (1994). Protein kinase regulation: insights from crystal structure analysis. Curr. Opin. Cell Biol. *6*, 239–246.

Navaza, J. (1992). AMoRe: a new package for molecular replacement. In Molecular Replacement: Proceedings of the CCP4 Study Weekend, E.J. Dodson, S. Gover, and W. Wolf, eds. (Daresbury, UK: SERC), pp. 87–90.

Otwinowski, Z. (1993). Oscillation data reduction program. In Proceedings of the CCP4 Study Weekend, L. Sawyer, N. Isaacs, and S. Burley, eds. (Daresbury, UK: SERC Daresbury Laboratory), pp. 56–62.

Russo, A.A., Jeffrey, P.D., and Pavletich, N.P. (1996). Structural basis of cyclin-dependent kinase activation by phosphorylation. Nat. Struct. Biol. *3*, 696–700.

Schindler, T., Sicheri, F., Pico, A., Gazit, A., Levitzki, A., and Kuriyan, J. (1999). Crystal structure of Hck in complex with a Src family–selective tyrosine kinase inhibitor. Mol. Cell *3*, this issue, 639–648.

Sicheri, F., Moarefi, I., and Kuriyan, J. (1997). Crystal structure of the Src family tyrosine kinase Hck. Nature *385*, 602–609.

Superti-Furga, G., Fumagalli, S., Koegl, M., Courtneidge, S.A., and Draetta, G. (1993). Csk inhibition of c-Src activity requires both the SH2 and SH3 domains of Src. EMBO J. *12*, 2625–2634.

Superti-Furga, G., and Courtneidge, S.A. (1995). Structure-function relationships in Src family and related protein tyrosine kinases. Bioessays *17*, 321–330.

Taylor, S.S., Buechler, J.A., and Yonemoto, W. (1990). cAMP-dependent protein kinase: framework for a diverse family of regulatory enzymes. Annu. Rev. Biochem. *59*, 971–1005.

Thomas, J.W., Ellis, B., Boerner, R.J., Knight, W.B., White, G.C., II, and Schaller, M.D. (1998). SH2- and SH3-mediated interactions between focal adhesion kinase and Src. J. Biol. Chem. *273*, 577–583.

Williams, J.C., Weijland, A., Gonfloni, S., Thompson, A., Courtneidge, S.A., Superti-Furga, G., and Wierenga, R.K. (1997). The 2.35 Å crystal structure of the inactivated form of chicken Src: a dynamic molecule with multiple regulatory interactions. J. Mol. Biol. *274*, 757–775.

Xu, W., Harrison, S.C., and Eck, M.J. (1997). Three-dimensional structure of the tyrosine kinase c-Src. Nature *385*, 595–602.

Yamaguchi, H., and Hendrickson, W.A. (1996). Structural basis for activation of the human lymphocyte kinase Lck upon tyrosine phosphorylation. Nature *384*, 484–489.

Zheng, J., Knighton, D.R., ten Eyck, L.F., Karlsson, R., Xuong, N., Taylor, S.S., and Sowadski, J.M. (1993). Crystal structure of the catalytic subunit of cAMP-dependent protein kinase complexed with MgATP and peptide inhibitor. Biochemistry *32*, 2154–2161.

Protein Data Bank Accession Number

Coordinates for the structures reported in this paper have been deposited in the Brookhaven Protein Data Bank (accession number 2SRC).